

The DC Microgrid with Energy Storage System

Rohit Kumar
Electrical Engineering Department
National Institute of Technology, Uttarakhand
Srinagar Garhwal, India
rohitkumarnit3010@gmail.com

Abstract: Powering frequently utilised DC loads like LEDs, laptops, and adjustable DC motor drives is where the DC microgrid truly shines. The DC microgrid, on the other hand, is constrained by substantial voltage differences between each converter and an unequal distribution of current among the converters, which leads to a lot of circulating current. The suggested distributed droop controller effectively lowers the constraints and provides an improved response in both transient and steady states. The distribution of currents from the equality line is also quantified on the inequality curve, which resembles the Lorenz curve in economics. In order to store extra power and then give it back to the bus, energy storage devices are also incorporated into DC buses. In this case, specific controller regulates the charging and discharging modes. While transitioning from charging to discharging and vice versa, the controller is likewise put to the test. The DC system is designed to accomplish the targeted purpose as a consequence.

Keywords: Current sharing, DAB converter, DC microgrid, energy storage integration, voltage regulation.

I. INTRODUCTION

The world now has the opportunity to switch to renewable and green energy and achieve carbon zero, as recommended in the IPCC Assessment Report[1], as a result of the slow destruction of the ozone layer and the inevitable demise of fossil fuels. The Emissions Gap Report[2] by the UN Environmental Program indicates that the world is on course to suffer a temperature increase of 3°C, which is double the goal set forth in the Paris Agreement. Ice melts as a result of this temperature increase, raising sea levels. As a consequence, a microgrid is created by fusing renewable energy sources like solar, wind, and hydro with an ac grid and energy storage systems. The type of the microgrid can be AC, DC, or hybrid, depending on the bus voltage. Nevertheless, the main problems with an AC microgrid are frequency and reactive power synchronization, skin effect, and a higher number of conversions to power typical DC loads like LEDs, computers, adjustable speed electric motors, and so on. Several people employ DC microgrids to get around the issues that ac microgrids provide. The main objectives of the DC microgrid are to minimize voltage regulation and control proportional current sharing among converters. There are a variety of methods for maintaining a steady bus voltage and lowering the circulating current among the converters. A crucial component of a DC microgrid is droop resistance, which evens out current distribution among converters and minimises load voltage regulation. The issue of selecting an appropriate droop resistance, on the other hand, is troublesome since a low droop resistance value leads to low load voltage regulation but substantial current distribution errors throughout the converters. On the other side, a high droop resistance causes poor load voltage regulation and low current distribution errors among the converters. As a consequence, a moderate droop resistance value is used to balance voltage regulation and current sharing.

All the existing controllers consist of three sub-controllers, namely primary, secondary and droop controllers. The secondary controller processes the intended reference voltage and related output current to produce the desired average output voltage and average output current, which are then processed by the appropriate controllers. The droop controller uses the secondary controller's results to adjust the primary controller's set voltage so that the secondary controller's results balance out the voltage drop across the droop resistance. Lastly, depending on the new reference voltage established by the droop controller, the main controller regulates the local output voltage and local output current of the converter.

There are primarily two classifications based on secondary control, namely centralized and decentralized control. With centralized control, a single central controller manages the whole converter connected to the DC microgrid by receiving all voltage and current information from the converter. When the central controller malfunctions and the system as a whole is rendered unusable, a problem occurs. It always results in a single point of failure. Each power converter's distributed controller is different. That finally resolves the issue with the centralized controller. In order to add the reference bus voltage to the average output current, the first method[3] in this control subtracts the voltage across the droop resistance from the sum of the average output current and a proportional constant. To implement inner loop control, the final reference voltage is contrasted with the output voltage. The second method[4] compares the average output voltage and current of each converter to its corresponding output voltage and current. Final errors are amplified by control transfer functions and then added to the desired output voltage. The output current and droop constant product are subtracted from the final set voltage before being compared to the output voltage before moving on to the inner loops. The third method[5] modifies the trend in order to take the average output voltage. In order to determine the average output voltage and compare it to the output voltage, it applies a consensus technique after receiving information on the output voltage and current of nearby converters. In the end, it is added to the reference voltage after calculating the current mismatch with the neighbouring output current. Before entering the inner loop, the new reference output voltage is subtracted from the product of the droop constant and output current. Every secondary distributed control has taken a predetermined droop value up until recently to keep the output voltage and current's slope constant. When the droop constant is high, the accuracy of the current sharing improves, but the voltage regulation deteriorates as well. Hence, a droop resistance is required to handle both load voltage control and the distribution of current among the converters. The fourth approach[6] is identical to the third one when these factors are taken into account. In this case, the output current is added to the product of the fixed droop value and output current, and the result is deducted from the reference output voltage. The slope of output voltage and current varies with the current mismatch. The procedure described in the following methods[7]–[14] averages all droop

constants, compares them to a reference droop constant, and then adds them to the corresponding droop constant. This technique's slope is also adjusting.

The bidirectional DC-DC converter[15]–[18] used for battery charging and discharging functions also complies with the droop control. The phase angle of the ac voltage at each terminal controls the charging and discharging operations of the dual active bridge (DAB) converter. When the phase angle is positive, energy moves from the battery to the bus side; conversely, when the phase angle is negative. In order to regulate the converter's conduction losses, the phase angle between the main and secondary voltages also controls the active power flow and inductor current RMS. The proposed theory goes through the two different controller types. In the charging mode, the conventional controller is used, and in the discharging mode, the distributed secondary controller that has been presented is used, together with source converters. For added battery protection against overcharging, the charging controller has a SoC estimation.

This article is organized in the following manner: Section-II presents a comprehensive overview of the proposed distributed controller. This is followed by a detailed explanation of the mathematical equations and V-I characteristics, which are used to illustrate the impact of varying droop resistance. Section-III focuses on the DAB controller, which is responsible for managing the battery throughout charging and discharging processes. Section-IV of this paper presents the simulation and findings that validate the controller mentioned in the preceding two sections. In conclusion, Section-V provides a summary of the expected objectives.

II. PROPOSED SECONDARY CONTROLLER

Droop resistance, which is discussed in section-I, is essential for improving the accuracy of current distribution among the converters and load voltage control. On the other hand, applying a suitable fixed droop value in accordance with the source as part of the traditional droop control approach is ineffective. The variable droop control modifies the droop values based on the difference between the output current and the mean output current or/and the mean output voltage and the reference voltage (Fig. 1).

In the proposed design, there are primarily three controllers.

i. **Secondary sub-controller:** It consists of voltage and current controllers that align the average output voltage to the reference voltage and the accompanying converter's instantaneous current to the average output current.

The output of the voltage controller:-

$$\delta_v = K_p^v(V_{ref} - \bar{v}_o) + K_i^v \int (V_{ref} - \bar{v}_o) dt \quad (1)$$

The output of the current controller:-

$$\delta_i = K_p^i(i_{o_i} - \bar{i}_o) + K_i^i \int (i_{o_i} - \bar{i}_o) dt \quad (2)$$

ii. **Droop sub-controller:** The secondary sub-controller's output is used to calculate fixed droop resistance, which is subsequently transformed to variable. The uneven distribution of current and significant voltage fluctuation across each load cause the variable droop resistance to spontaneously vary. The output of the secondary voltage and current controllers is added to the reference voltage and deducted from the converter current, which is multiplied by the variable droop resistance.

The variable droop resistance: -

$$r_{d_i} = R_D - [K_p^i(i_{o_i} - \bar{i}_o) + K_i^i \int (i_{o_i} - \bar{i}_o) dt] + [K_p^v(V_{ref} - \bar{v}_o) + K_i^v \int (V_{ref} - \bar{v}_o) dt] \quad (3)$$

New set voltage for the primary controller:-

$$V_{DC_i}^* = V_{ref} - r_{d_i}i_{o_i} + K_p^v(V_{ref} - \bar{v}_o) + K_i^v \int (V_{ref} - \bar{v}_o) dt + K_p^i(i_{o_i} - \bar{i}_o) + K_i^i \int (i_{o_i} - \bar{i}_o) dt \quad (4)$$

Where, i shows the parameter values for i^{th} converter

$V_{DC_i}^*$ = Reference primary voltage

V_{ref} = Reference DC bus voltage

r_{d_i} = Variable droop resistance

i_{o_i} = Output current

\bar{i}_o = Average DC output current

\bar{v}_o = Average DC output voltage

K_p^i & K_p^v = Proportional constants of secondary current and voltage controllers, respectively

K_i^i & K_i^v = Integral constants of secondary current and voltage controllers, respectively.

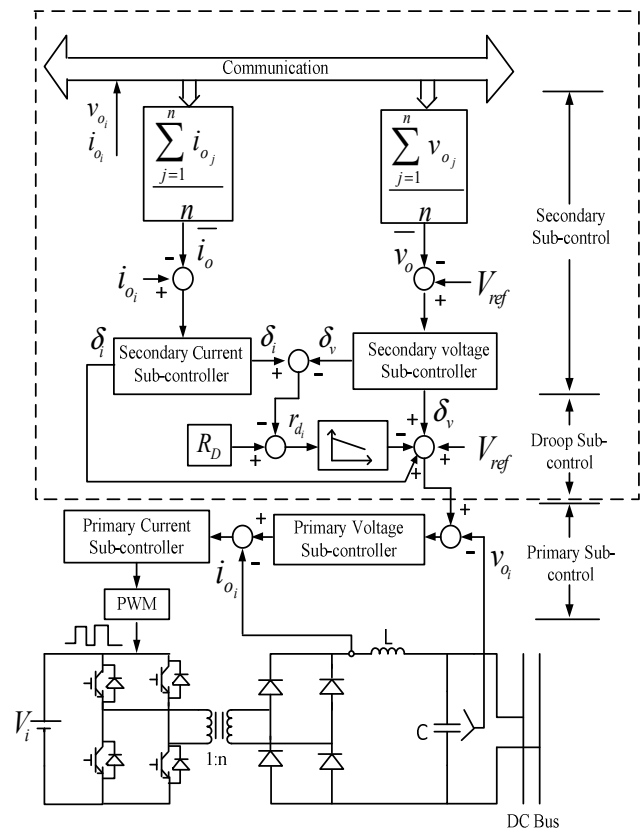


Fig. 1: Proposed distributed secondary control

iii. **Primary sub-controller:** A regular controller that is commonly utilised to close the loop on a DC-DC converter. It also features voltage and current regulators that keep the output load voltage constant with the droop controller's new reference voltage while keeping the output current within a defined range.

Equation (4) generates the reference voltage for the primary controller after deducting the voltage drop caused by the variable droop resistance. To adjust the reference voltage to the required value, both voltage and current correction components are included at the end. The difference between variation in droop resistance (δr_i) and fixed droop resistance (R_D) is known as variable droop resistance (r_{d_i}). The difference between two correction terms produced from

secondary voltage and current controllers is referred to as the change in droop resistance (δr_i).

It can be seen from the preceding equations that the outputs of both secondary voltage and current controllers have a dual purpose:

- (i) They function as voltage shifting terms, shifting the primary control set voltage to the desired value while compensating the voltage drop caused by variable droop resistance.
- (ii) They also contribute to the variable droop resistance, which varies whenever there is unequal distribution of current among converters and significant voltage regulation across each load.

Now, there are two different degrees of freedom in the variable droop resistance (r_{d_i}). The following modifications (Fig.2) are included in it:

- (i) Variation in output current compared to the average output current.
- (ii) Difference between the reference bus voltage and the average output voltage.

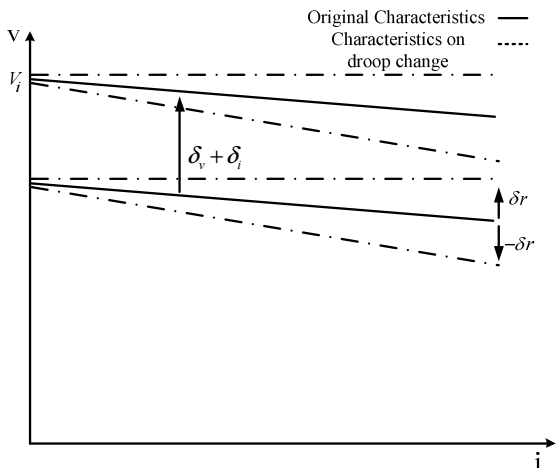


Fig.2: Voltage-current characteristics of the suggested controller

The updated reference voltage ($v_{DC_i}^*$) acquired after processing via both secondary and droop controllers is sent into the converter's primary controller. It has an internal voltage and current controller that generates PWM pulses to drive the converter. This control incorporates a full-bridge isolated DC-DC converter that employs the phase-shifted PWM method.

III. DAB CONTROLLER

The controller (Fig.3) to run the dual active bridge converter is divided into two parts. Each part is meant for different modes. For charging mode, the phase delay angle is positive, i.e., the primary voltage leads the secondary voltage and power flow from the bus side to the battery side. The controller is a conventional one. It senses the voltage across the battery and its current and processes it in respective controllers to provide the gate pulse to the switches of the converter. A state of charge (SoC) checker is kept in its path to prevent the battery from overcharging. Whenever SoC reaches 100%, the converter stops working, and the battery is protected against deterioration caused by overcharging.

But, when the mode is switched to the discharging mode, the phase delay angle is negative, indicating that the secondary voltage leads the primary voltage, and power flows from the battery side to the bus side. The distributed droop controller, as explained in section 2, is utilised in this mode. It calculates the average output voltages and currents and compares them

to the reference bus voltage and local output current through secondary controller. The final outcome of the secondary controller is used as a reference by the primary controller. Local voltage and current controllers are included in the primary controller, which compares local output voltage to the secondary controller's output and local output current to the primary voltage controller's output. The primary controller's output is used to drive the PWM circuit, which operates the switches of both the primary and secondary sides of the high-frequency transformer.

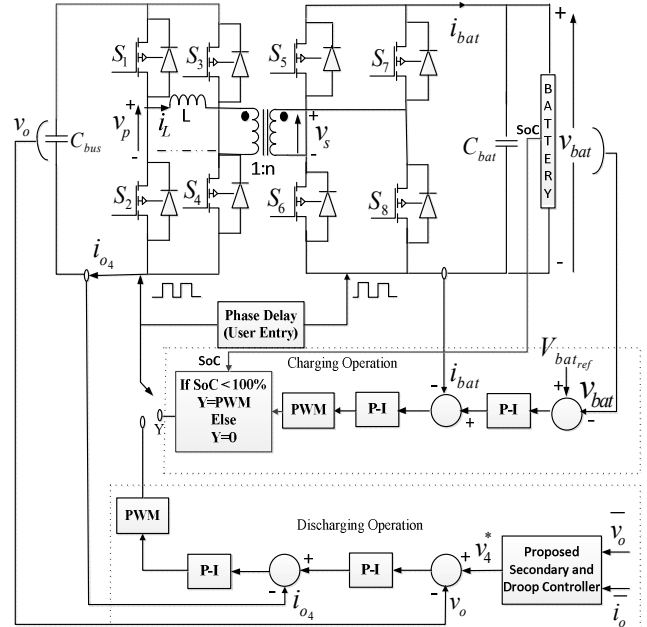


Fig.3: The controller for the DAB converter

IV. RESULT AND DISCUSSION

The proposed topology (Fig.4) is simulated in MATLAB/Simulink R2020a. The DC bus is linked to three full-bridge isolated DC-DC converters with a common central load and local loads attached to each converter. Through a DAB converter, the surplus DC bus power is stored in the battery and later utilised during dark times. A 3-level PWM converter connects the AC grid to the bus, resulting in minimal harmonic content in grid current that is in phase with the grid voltage.

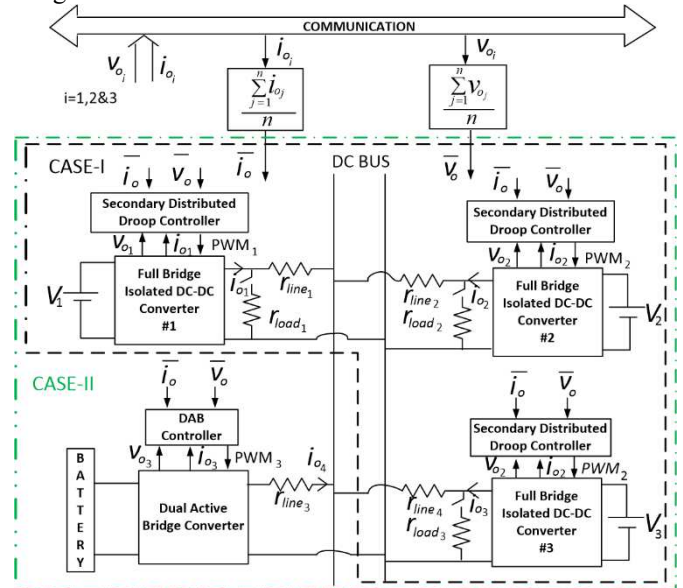


Fig.4: Proposed Topology

Case I: Equal current distribution and low voltage regulation are investigated.

Following the suggested controller outlined in section-II, isolated DC-DC converters feed the central load linked to the bus and local loads attached to each converter. The transient and steady state outputs are contrasted in this scenario, as well as a full review of the suggested controller.

Case-I.A: When only the primary controller works.

The secondary and droop controllers are eliminated in this scenario, leaving just the primary controller to be investigated (shown in Fig.5). The load voltages are suffering from overshoots and undershoots (Fig.6). There is a significant potential difference between each load that shows poor voltage regulation. The current distribution among each converter is unequal, and the differences of output current also represent a large gap (Fig.7). The output current's inequality curve shows a large deviation from the absolute equality line, which supports the major unequal current sharing among the converter (Fig.8).

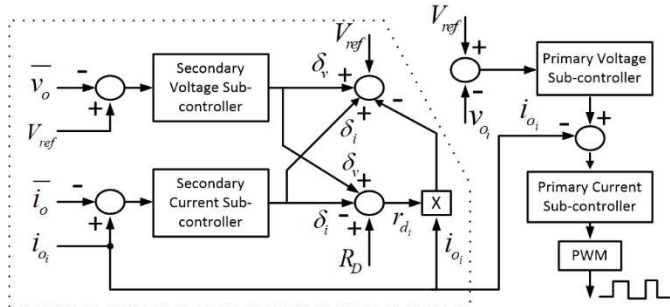


Fig.5: The controller without the proposed scheme used in case-I.A

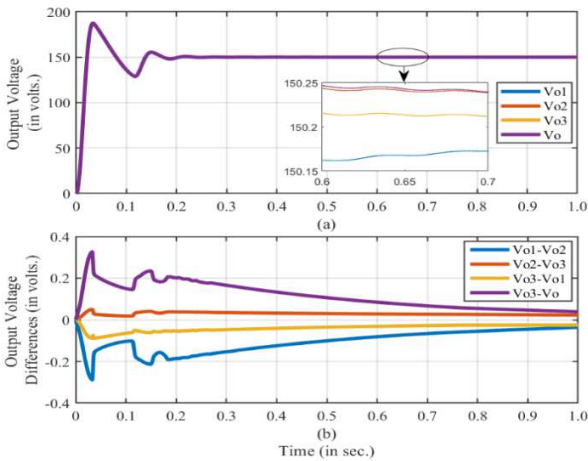


Fig.6: (a).The output voltage across each load (b).Output voltage differences for case-I.A.

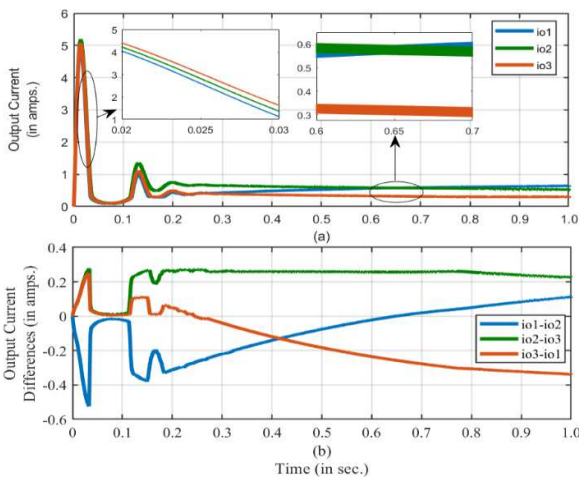


Fig.7: (a). Output Current of each converter (b). Differences of output current for case-I.A

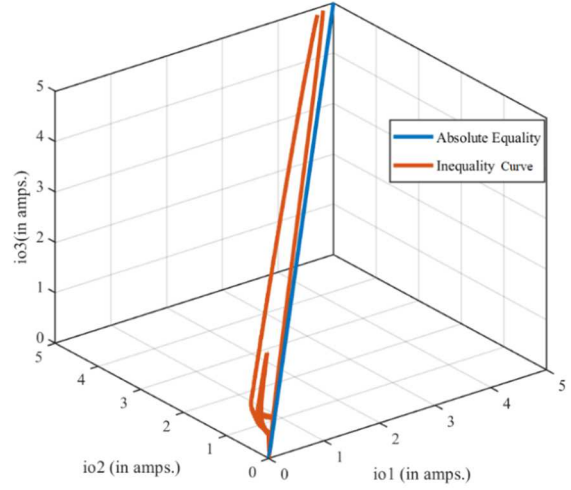


Fig.8: Inequality curve for case-I.A

Case-I.B: When the proposed secondary and droop controllers are included.

When proposed secondary voltage and current controllers are included so that the droop resistance varies with two degrees of freedom, namely outputs of secondary voltage and current controllers, these two outputs are considered as the correction terms, which perform the dual task of voltage shifting terms and changing the droop resistance dynamically (Fig.9).

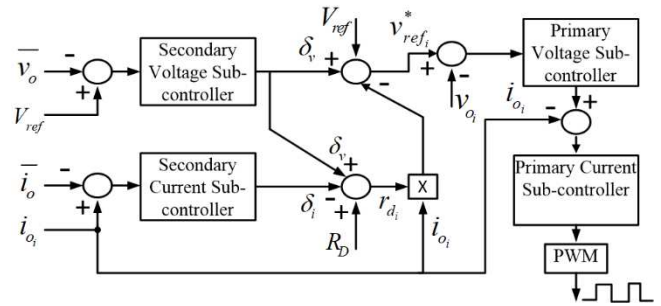


Fig.9: The secondary distributed controller used in case-I.B

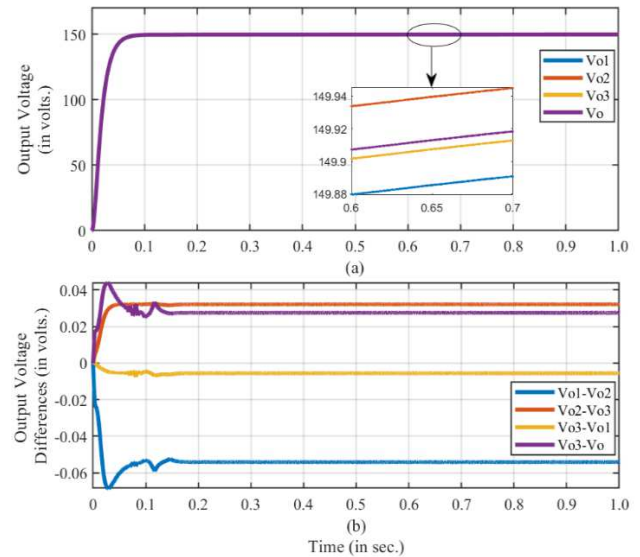


Fig.10: (a). The output voltage across each load (b). Output voltage differences for case-I.B

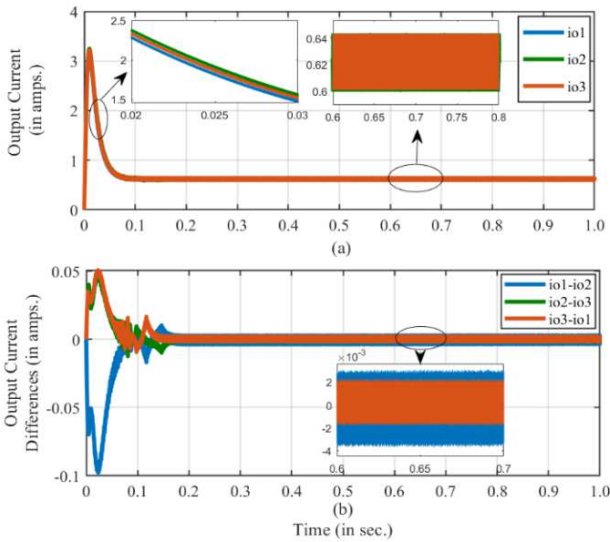


Fig.11 (a). Output Current of each converter (b). Differences of output current for case-I-B

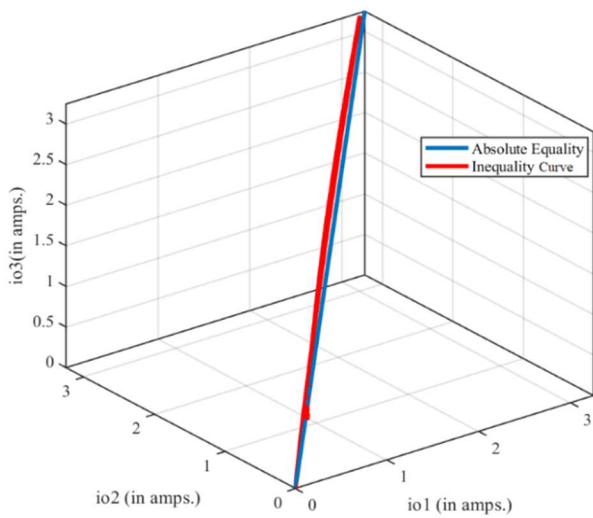


Fig.12: Inequality curve for case-I-B

The transient and steady state responses of output voltages and output currents demonstrate the impacts (Figs.10 and 11). The output voltages are not suffering from overshoot and undershoot as well as the differences in output voltages also show minimum value, resulting in low voltage regulation across loads (Fig.10). The output current is nearly equalised with little overshoot in the case of current distribution (Fig.11(a)). Furthermore, the decreased difference in output currents (Fig.11(b)) indicates that the current distribution among the converters is more uniform. The output current inequality curve (Fig.12) displays the best outcome of all the scenarios. It is almost at the line of absolute equality.

Case-II: Integration of Energy Storage System to store surplus DC power

As stated in section-III, the dual active bridge converter is integrated with the system to feed the energy storage devices and extract their energy later. The phase angle between the primary and secondary voltages of a high frequency transformer determines the direction of power flow. When the phase difference is positive, the primary voltage leads the secondary voltage. Chargers for energy storage devices are turned on. When the phase difference is negative, the scenario is reversed.

In this case, the battery switches from charging to discharging mode at $t=1.0\text{sec}$. When the battery is in charging mode, the DAB converter follows the conventional controller. But, when it is in discharging mode, the DAB converter follows the distributed droop controller to equalize current distribution among the converters and reduce load voltage regulation.

When the bus side voltage is leading to the battery side voltage, the battery starts charging. As the battery side voltage is made leading with respect to the bus side voltage at $t=1.0\text{sec}$, the battery switches to discharging mode as shown in Fig.13. The DAB converter's output current is negative in the charging mode, and the battery switches to the discharging mode, the DAB converter's output current becomes equal to the other converter's output current in the discharging mode (Fig.14(a)). The output voltage is 150V, but at $t=1.0\text{sec}$, it rises and then settles again at 150V (Fig.14(b)). The output power is 390 watts in the charging mode, but it drops to 225 watts in the discharging mode (Fig.15).

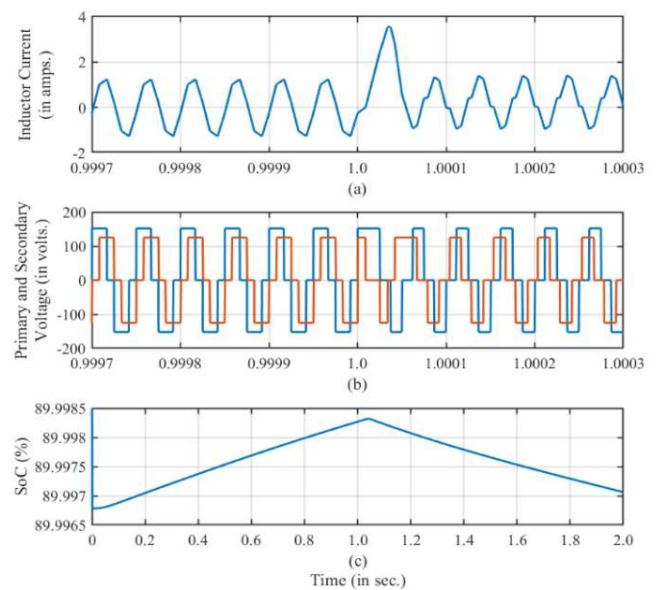


Fig.13: (a).Inductor current (b).primary and secondary voltage referred to the low voltage side of the high-frequency transformer (c).battery's SoC obtained in case-II

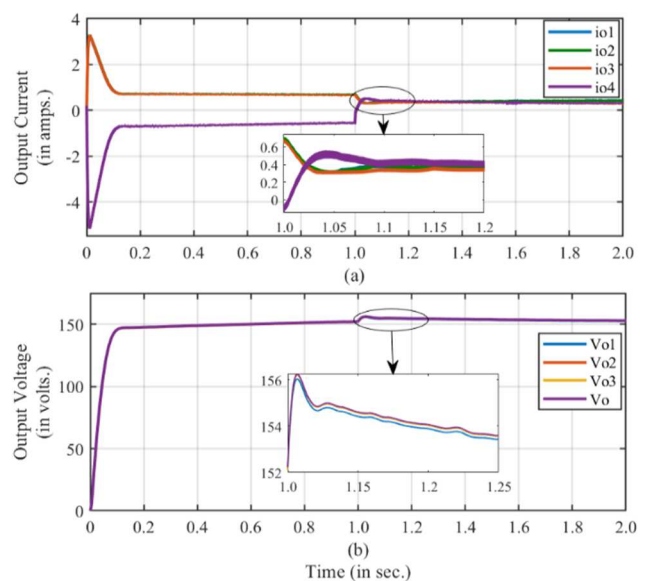


Fig.14: (a). Output currents and (b) output voltage across each load in case-II

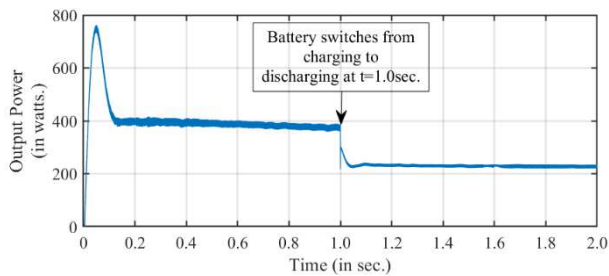


Fig.15: The output power obtained in case-II

V. CONCLUSION

This paper describes the comprehensive DC microgrid structure that integrates renewable sources and battery to feed DC loads. In order to level off the current distribution among the converters and minimise load voltage regulation, the DC sources connected to the bus through a full-bridge isolated DC-DC converter adhere to the suggested distributed secondary controller. The proposed controller is acting efficiently in both transient and steady states. The distribution of currents among the converters are also quantized on the inequality curve which is analogous to the Lorenz curve in economics. To store the excess power of the bus the battery system is connected, which may power the load during night time. The battery is connected to the bus through a dual active bridge converter that follows the conventional controller in the charging mode and obeys the proposed distributed controller in the discharging mode. The proposed system is flexible in the instant conversion of modes from charging to discharging mode and vice-versa. Hence, the proposed system is designed to feed DC loads, fulfilling their objectives.

REFERENCES

- [1] "Climate Change 2022: Impacts, Adaptation and Vulnerability. Working Group II Contribution to the IPCC Sixth Assessment Report," 2022.
- [2] UNEP Copenhagen Climate Centre, "Emissions Gap Report 2021."
- [3] S. Anand, B. G. Fernandes, and J. Guerrero, "Distributed Control to Ensure Proportional Load Sharing and Improve Voltage Regulation in Low-Voltage DC Microgrids," *IEEE Trans. Power Electron.*, vol. 28, no. 4, pp. 1900–1913, Apr. 2013, doi: 10.1109/TPEL.2012.2215055.
- [4] X. Lu, J. M. Guerrero, K. Sun, and J. C. Vasquez, "An improved droop control method for dc microgrids based on low bandwidth communication with dc bus voltage restoration and enhanced current sharing accuracy," *IEEE Trans. Power Electron.*, vol. 29, no. 4, pp. 1800–1812, 2013.
- [5] V. Nasirian, S. Moayedi, A. Davoudi, and F. L. Lewis, "Distributed cooperative control of DC microgrids," *IEEE Trans. Power Electron.*, vol. 30, no. 4, pp. 2288–2303, 2014.
- [6] V. Nasirian, A. Davoudi, F. L. Lewis, and J. M. Guerrero, "Distributed Adaptive Droop Control for DC Distribution Systems," *IEEE Trans. Energy Convers.*, vol. 29, no. 4, pp. 944–956, Dec. 2014, doi: 10.1109/TEC.2014.2350458.
- [7] P. Wang, X. Lu, X. Yang, W. Wang, and D. Xu, "An Improved Distributed Secondary Control Method for DC Microgrids With Enhanced Dynamic Current Sharing Performance," *IEEE Trans. Power Electron.*, vol. 31, no. 9, pp. 6658–6673, Sep. 2016, doi: 10.1109/TPEL.2015.2499310.
- [8] A.-C. Braitor, G. C. Konstantopoulos, and V. Kadiramanathan, "Current-Limiting Droop Control Design and Stability Analysis for Paralleled Boost Converters in DC Microgrids," *IEEE Trans. Control Syst. Technol.*, vol. 29, no. 1, pp. 385–394, Jan. 2021, doi: 10.1109/TCST.2019.2951092.
- [9] B. Zhang, F. Gao, Y. Zhang, D. Liu, and H. Tang, "An AC-DC Coupled Droop Control Strategy for VSC-Based DC Microgrids," *IEEE Trans. Power Electron.*, vol. 37, no. 6, pp. 6568–6584, Jun. 2022, doi: 10.1109/TPEL.2022.3141096.
- [10] P. Li *et al.*, "Reduced-Order Modeling and Comparative Dynamic Analysis of DC Voltage Control in DC Microgrids Under Different Droop Methods," *IEEE Trans. Energy Convers.*, vol. 36, no. 4, pp. 3317–3333, Dec. 2021, doi: 10.1109/TEC.2021.3076438.
- [11] N. Ghanbari and S. Bhattacharya, "Adaptive Droop Control Method for Suppressing Circulating Currents in DC Microgrids," *IEEE Open Access J. Power Energy*, vol. 7, pp. 100–110, 2020, doi: 10.1109/OAJPE.2020.2974940.
- [12] Y. Zhang, X. Qu, M. Tang, R. Yao, and W. Chen, "Design of Nonlinear Droop Control in DC Microgrid for Desired Voltage Regulation and Current Sharing Accuracy," *IEEE J. Emerg. Sel. Top. Circuits Syst.*, vol. 11, no. 1, pp. 168–175, Mar. 2021, doi: 10.1109/JETCAS.2021.3049810.
- [13] R. Kumar and M. K. Pathak, "Distributed droop control of dc microgrid for improved voltage regulation and current sharing," *IET Renew. Power Gener.*, vol. 14, no. 13, pp. 2499–2506, Oct. 2020, doi: 10.1049/iet-rpg.2019.0983.
- [14] R. Kumar and M. K. Pathak, "Control of DC Microgrid for Improved Current Sharing and Voltage Regulation," in *2020 3rd International Conference on Energy, Power and Environment: Towards Clean Energy Technologies*, Mar. 2021, pp. 1–4, doi: 10.1109/ICEPE50861.2021.9404421.
- [15] J. Wu, Y. Li, X. Sun, and F. Liu, "A New Dual-Bridge Series Resonant DC–DC Converter With Dual Tank," *IEEE Trans. Power Electron.*, vol. 33, no. 5, pp. 3884–3897, May 2018, doi: 10.1109/TPEL.2017.2723640.
- [16] O. Cipriano da Silva, F. L. Tofoli, D. Honorio, L. H. Barreto, and D. de S. Oliveira, "Single-Phase Isolated AC-AC Converters Based on the Dual Active Bridge Converter," *IEEE Trans. Ind. Electron.*, vol. 69, no. 6, pp. 5680–5689, Jun. 2022, doi: 10.1109/TIE.2021.3088363.
- [17] C. Sun, X. Zhang, J. Zhang, M. Zhu, and J. Huang, "Hybrid Input-Series–Output-Series Modular DC–DC Converter Constituted by Resonant and Nonresonant Dual Active Bridge Modules," *IEEE Trans. Ind. Electron.*, vol. 69, no. 1, pp. 1062–1069, Jan. 2022, doi: 10.1109/TIE.2021.3055175.
- [18] F. D. Esteban, F. M. Serra, and C. H. De Angelo, "Control of a DC-DC Dual Active Bridge Converter in DC Microgrids Applications," *IEEE Lat. Am. Trans.*, vol. 19, no. 8, pp. 1261–1269, Aug. 2021, doi: 10.1109/TLA.2021.9475856.